Ecological Indicators 61 (2016) 404–412

Contents lists available at ScienceDirect

Ecological Indicators

journal homepage: www.elsevier.com/locate/ecolind

Multiple afforestation programs accelerate the greenness in the 'Three North' region of China from 1982 to 2013

Yao Zhang[a,b], Changhui Peng[a,c,d], Weizhong Li[a,*], Liuxi Tian[a,e], Qiuan Zhu[a,d], Huai Chen[f], Xiuqin Fang[g], Geli Zhang[b], Guobin Liu[d], Xingmin Mu[d], Zhanbin Li[d], Shiqing Li[d], Yanzheng Yang[a], Jie Wang[b], Xiangming Xiao[b,h]

[a] College of Forestry, Northwest A&F University, Yangling, Shaanxi 712100, China
[b] Department of Microbiology and Plant Biology and Center for Spatial Analysis, University of Oklahoma, Norman, OK 73019, USA
[c] Center of CEF/ESCER, Department of Biological Science, University of Quebec at Montreal, Montreal H3C 3P8, Canada
[d] State Key Laboratory of Soil Erosion and Dryland Farming on the Loess Plateau, Northwest A&F University, Yangling, Shaanxi 712100, China
[e] Department of Geological Sciences, University of Texas at San Antonio, TX 78249, USA
[f] Key Laboratory of Mountain Ecological Restoration and Bioresource Utilization & Ecological Restoration Biodiversity Conservation Key Laboratory of Sichuan Province, Chengdu Institute of Biology, Chinese Academy of Sciences, Chengdu 610041, China
[g] School of Earth Science and Engineering, Hohai University, Nanjing 210098, China
[h] Institute of Biodiversity Sciences, Fudan University, Shanghai 200433, China

ARTICLE INFO

Article history:
Received 26 June 2015
Received in revised form
20 September 2015
Accepted 24 September 2015
Available online 11 November 2015

Keywords:
Planted forest
Ecological restoration
NDVI
Arid and semi-arid regions
GIMMS
GIMMS 3g
MODIS

ABSTRACT

China has launched multiple afforestation programs since 1978, including the 'Three North' Shelterbelt Development Program (TNSDP), the Beijing–Tianjin Sand Source Control Program (BSSCP), the Nature Forest Conservation Program (NFCP), and the Grain to Green Program (GTGP). These programs focus on local environment restoration by planting trees in semi-arid and arid regions and by protecting natural forests. However, the effectiveness of these programs has been questioned by several previous studies. Here, we report an increasing trend of greenness in this region using the satellite-retrieved normalized difference vegetation index (NDVI) from GIMMS, GIMMS-3g and MODIS datasets in the past 32 years. The NDVI increase for the 'Three North' region was 0.28%–0.38% yr^{-1} in 1982–2000 and 0.86%–1.12% yr^{-1} in 2000–2013, which is much higher than the country's means of 0.060%–0.063% yr^{-1} and 0.27%–0.30% yr^{-1}, respectively. Most of the increase occurred in low and sparsely vegetated areas; and enlarged the moderate vegetated area (growing season mean NDVI above 0.5) from 16.5% to 25.7% for the two time periods, respectively. We also analyzed changes in the length of the growing season and the climate conditions including temperature, precipitation and two drought indices. However, these environmental factors cannot completely explain the changes in vegetation activity. Our study suggests these multiple afforestation programs contributed to the accelerated greening trend in the 'Three North' region and highlight the importance of human intervention in regional vegetation growth under climate change condition.

1. Introduction

An increasing vegetation activity has been reported in the northern hemisphere as a result of the global climate change (Nemani et al., 2003; Piao et al., 2006a; Xu et al., 2013). Many studies have investigated the climate change impact on the vegetation growth in China for the past decades (Peng et al., 2011; Piao et al., 2009). However, as vegetation growth is influenced by both environmental drivers (e.g., climate change) and human activities, the role of human played in the changing environment still remains less studied (Piao et al., 2015). During the past decades, the interaction between natural ecosystems and humans has intensified with increasing human productivity (Vitousek et al., 1997), understanding human impacts on vegetation change is one of the key challenges facing our research community as it seeks to solve current and future environmental problems (Falkowski et al., 2000).

Along with rapid economic growth, China is facing various environmental problems, including desertification, sandstorms, soil water erosion, and land degradation in dry northern regions (Liu and Diamond, 2005). Since 1978, China has launched a series of ecological restoration programs to mitigate these increasingly devastating environment problems, particularly in the 'Three North'

* Corresponding author.
E-mail address: wzhli6465@163.com (W. Li).

http://dx.doi.org/10.1016/j.ecolind.2015.09.041
1470-160X/

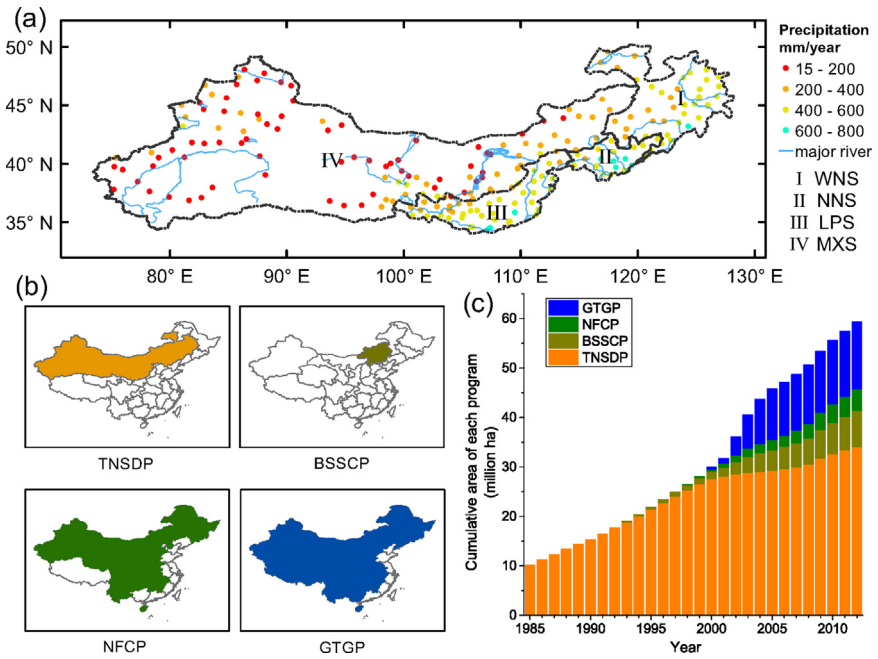

Fig. 1. (a) The location of the Three North region. The dots represent the annual mean precipitation from weather stations beginning in 1951. (b) Spatial extent of the four major ecological restoration programs in China since 1978. (c) Cumulative afforested area for each ecological restoration program from 1985 to 2012. The TNSDP began in 1978, but the annual planted area could not be obtained until 1986; therefore, the total planted area from 1978 to 1985 is shown for 1985. The GTGP and NFCP are countrywide restoration programs, and only provinces in our study area, i.e., Heilongjiang, Jilin, Liaoning, Inner Mongolia, Beijing, Tianjin, Hebei, Shanxi, Shaanxi, Ningxia, Gansu, Xinjiang and Qinghai are included in our statistics.

region (Northern part of China, see Fig. 1) (Yin and Yin, 2010). The 'Three North' Shelterbelt Development Program (TNSDP), which was initiated in 1978, is the largest afforestation program in the world (Li et al., 2012). Aimed at planting protective forests in arid and semi-arid areas, this program has been in place for more than three decades and will continue until 2050. The subsequent Beijing–Tianjin Sand Source Control Programs (BSSCP), which aims to protect against sandstorms through afforestation (Wu et al., 2013), the Natural Forest Conservation Program (NFCP), which aims at protecting natural forests through logging bans, and the Grain to Green Program (GTGP), which targets to convert farmland into forests and grasslands (Jia et al., 2014; Liu et al., 2014), have all been implemented in the 'Three North' region since 2000. Although enhanced vegetation had successfully combated the desertification and dust storms (Zhang et al., 2012; Fan et al., 2014; Piao et al., 2005; Tan and Li, 2015), sequenced carbon in both above ground biomass and soil (Deng et al., 2014; Song et al., 2014; Zhou et al., 2014), cooled down the surface temperature (Peng et al., 2014), and showed a positively feedback to the regional environment (Jiang et al., 2015; Zhang et al., 2014), the effectiveness of planting trees has been questioned by other researchers because of low precipitation in these dry regions (Cao, 2008; Cao et al., 2010; Ma et al., 2013; Sun et al., 2006). Cao (2008) even asserted that afforestation would lead to wind erosion but was rebutted by other scholars (Yang and Ci, 2008). Alongside with the global climate change, increasing drought frequency also offset the effectiveness of these programs (Wu et al., 2014). However, these studies often focused on a small region or used single dataset to evaluate the vegetation activity in a short period, the representative of these studies are limited due to the very large temporal and spatial span of the afforestation programs. A recent study by He et al. (2015) investigated the vegetation change using the satellite images in the 'Three North' region but focused more on the environmental effects. The overall contribution of multiple afforestation programs are still less investigated. How to discriminate the effects of climate change from human afforestation remains unclear.

In this study, we investigated the effectiveness of ecological restoration programs on vegetation activities in the 'Three North' region over the past three decades, using the satellite-derived normalized difference vegetation index (NDVI) from Global Inventory Modeling and Mapping Studies (GIMMS, 1982–2006), GIMMS third generation (GIMMS 3g, 1982–2012) and Moderate Resolution Imaging and Spectroradiometer (MODIS, 2000–2013) datasets. Specifically, we compared the NDVI trends based on multiple methods in two periods: 1982–2000 and 2000–2013. The breakpoint in 2000 was selected because the three later ecological restoration programs (GTGP, NFCP, and BSSCP) were implemented around 2000 following the TNSDP. Additionally, the MODIS NDVI dataset begins in 2000 and a breakpoint in 2000 was also found in analysis. To better understand the human intervention in our study area, the statistical data of afforestation area was obtained from the China Forestry Administration. The trend of the length of growing season (LGS) and two drought indices were also calculated to indicate the effect from climate change. The final conclusion was drawn through the comparison between two study periods and comparison with other parts of China.

2. Materials and methods

2.1. Study area

The 'Three North' region includes the northwestern, central north and northeastern part of China. The geographical extent ranges from 73°27′ E to 128°13′ E, 34°2′ N to 50°11′ N. It is constituted of 13 provinces and accounts for 42.4% of the total land area in China (Fig. 1a). The program region is further divided into four subregions including western Northeast China (WNS), northern North China (NNS), the Loess Plateau (LPS) and Mongolia–Xinjiang subregions (MXS). This partitioning was adopted from the project plans and were categorized by multiple characteristics, including soil properties, vegetation, climate, and program objectives

(China Forestry Administration, Bureau of Three North Shelterbelt Development Program, 1987). The annual precipitation for most area is less than 600 mm. The forest cover was only 5.05% in 1978 when the programs was initiated and this region was jeopardized by drought, sandstorms, and desertification (Wang et al., 2010).

Because (1) no accurate afforestation map is public available, (2) these programs also protected forest through logging bans, shrub and grass planting, our analysis did not focus on exclusive forest area but the whole 'Three North' region.

2.2. NDVI datasets

The NDVI is related to photosynthetically active radiation absorbed by canopies; therefore, it is a good indicator of surface vegetation condition (Huete et al., 2002; Pinzon and Tucker, 2014). The positive and negative trends of NDVI are referred to as 'greening' and 'browning', respectively (Alcaraz-Segura et al., 2010). Three NDVI datasets were used in our study including Global Inventory Modeling and Mapping Studies (GIMMS 1982–2006), Moderate Resolution Imaging and Spectroradiometer (MODIS, 2000–2013) and the GIMMS third generation (GIMMS 3g, 1982–2012). A previous study found a large difference between the GIMMS and GIMMS 3g dataset in the north hemisphere and suggest that GIMMS and MODIS can be used in conjunction (Guay et al., 2014). To prove the accelerated greening trend is not caused by dataset artifact, we used all these three datasets for analysis. The GIMMS 3g dataset was used as a complementary of our research and most result are shown in the supplementary material. Data from these 32 years were divided into two periods: 1982–2000 and 2000–2013 (2000–2012 for GIMMS 3g dataset). We analyzed the trends and phenological change for the two periods separately.

The GIMMS NDVI dataset from 1982 to 2006 was acquired from the Global Land Cover Facility at the University of Maryland. This dataset, with a spatial resolution of 8 km and a temporal resolution of 15 days, was obtained by AVHRR instruments from NOAA satellite series 7, 9, 11, 14, 16 and 17. The maximum value composites (MVC) were used to eliminate cloud and aerosol effects and were then aggregated into half-month composites. This dataset was corrected for calibration and view geometry, and it has been widely applied in global and regional studies (Peng et al., 2010; Tucker et al., 2005).

The MODIS C5 NDVI dataset from 2000 (February) to 2013 was acquired from the NASA Land Processes Data Active Archive Center (LP DAAC). The $0.05^\circ \times 0.05^\circ$ spatial resolution and 16-day frequency climate model grid (CMG) (MOD13C1) dataset was used in our study because it has a similar spatial resolution to the GIMMS dataset (approximately 5 km). The MODIS dataset has been widely used in various aspects (Kilpatrick et al., 2015; Rahimi et al., 2015; Yao et al., 2015), and the accuracy of the NDVI dataset has been tested worldwide (Huete et al., 2002).

The GIMMS 3g NDVI dataset is an updated version of the previous GIMMS NDVI version (Pinzon and Tucker, 2014), the spatial resolution of this dataset is one-twelfth of a degree and the temporal resolution is half a month.

The quality of the 16-day NDVI data from MODIS can be assessed through a QA layer where each $0.05^\circ \times 0.05^\circ$ pixel corresponds to a 16-bit quality flag. This 16-bit number provides information on how the NDVI value is processed and potential data quality issues. A pixel is considered corrupted by clouds when 'Adjacent cloud detected' (bit 8) and 'Mixed clouds' (bit 10) equals to '1' (Yes). A pixel's aerosol quality is described by 'Aerosol quantity' (bit 6–7) and is considered corrupted when it equals '00' (Climatology) or '11' (High) (Vermote and Vermeulen, 1999).

2.3. Vegetation growth trend analysis

Three methods were used to analyze the vegetation growth trend for the 'Three North' region, including the least square regression, the Mann–Kendall test and Sen's slope estimator, and the Breaks For Additive Season and Trend (BFAST) algorithm.

The Mann–Kendall test is a non-parametric significance test to statistically assess whether there is a monotonic upward or downward trend of a variable overtime (Kendall, 1975; Mann, 1945). It measures the ranks of observations rather than actual values, and it has low sensitivity to abrupt changes. This test was originally applied in hydrological analyses and more recently has been used with NDVI data (de Jong et al., 2011; Sobrino and Julien, 2011). The magnitude of the slope of the trend was estimated with Sen's slope (Sen, 1968). It is a robust estimate of the magnitude of monotonic trends and insensitive to outliers. Therefore, the Sen's slope may provide an accurate estimate of the regression slope for skewed and heteroskedastic data. The calculation of the Mann–Kendall test and Sen's slope can be found in Appendix.

For the entire study area and the four subregions, mean NDVI for the growing season (May to September, as reported by Piao et al., 2006b) was calculated for each year. For the two time periods (1982–2000 for GIMMS and GIMMS 3g, and 2000–2013 for MODIS, 2000 to 2012 for GIMMS 3g), the least square regression and Mann–Kendall test were conducted for each pixel. Only pixels with a significant trend ($\alpha < 0.1$) in the Mann–Kendall test were used to calculate Sen's slope.

We also used the BFAST algorithm to analyze the NDVI time series from 1982 to 2013. This algorithm uses an iteratively piecewise linear regression model and a seasonal decomposition model to obtain the seasonal, trend, and remainder components of the NDVI time series. The model is described as Eq. (1)

$$Y_t = T_t + S_t + R_t, \quad t = 1, \ldots, n \tag{1}$$

where Y_t is NDVI observation at time t. T_t, S_t, and R_t are the trend, seasonal, and remainder components of the corresponding observation, respectively. Numbers and locations of potential breakpoints in T_t and S_t are detected by a least squares residual method and are iterated until unchanged. This algorithm was developed by Verbesselt et al. (2010a,b) in R (http://bfast.R-Forge.R-project.org/). Because this method took the seasonal variation into consideration, the mean NDVI value for the whole vegetated area were calculated for each scene first, after which, the BFAST method was applied with the same set of parameters ($h = 0.15$, season = 'dummy', max. iter = 5).

2.4. Retrieval of phenological changes from satellite data

TIMESAT software (Version 3.1, http://www.nateko.lu.se/timesat/timesat.asp) was used for retrieving the start of the season (SOS) and the length of growing season (LGS) for three NDVI datasets. It fits a smooth curve to the NDVI time series using Savitzky–Golay filtering, the asymmetrical Gaussian method or the double logistic method (Jönsson and Eklundh, 2004). In our study, the Savitzky–Golay filter was used, and the threshold to derive the SOS and end of season (EOS) was 20% between the minimum and maximum values. After retrieving the LGS for each year, a least square regression was applied to each pixel to calculate the trend of phenological change. Because some pixels may fail to extract a valid SOS and LGS (e.g. LGS less than zero or greater than 365 days), only pixels with more than half of the valid SOS and LGS produced a trend value. It should be noted that this process may introduce bias for the very sparse vegetated area.

2.5. Drought indices

Both the Palmer Drought Severity Index (PDSI) and Standardized Precipitation Index (SPI) were used to indicate the water limitation. The PDSI is a measure of the cumulative deviation in the surface water balance and was designed to assess drought severity in semi-arid regions (Palmer, 1965). The SPI is designed to quantify the precipitation deficit based on a long-term precipitation record for a desired period. This long-term record is fitted to a probability distribution and then standardized so that the mean SPI for a given period is zero (McKee et al., 1993).

The PDSI data were obtained from the National Center for Atmospheric Research. This dataset has a spatial resolution of 2.5° × 2.5° Areas with a growing season mean NDVI below 0.1 were masked for analysis. The PDSI varies roughly from −10 (dry) to 10 (wet); values between −0.5 and 0.5 are considered near normal, values from −2 to −2.99 are considered moderate drought, values from −3 to −3.99 are considered severe drought, and values below −4 are considered extreme drought (Palmer, 1965).

The SPI calculation was based on monthly precipitation data acquired from weather stations since 1951. Stations located on bare ground with no vegetation were screened for analysis. The SPI can be qualified on different time scales. In our study, 6-month scales were used to detect medium-term droughts. The SPI values between −0.99 and 0.99 are considered near normal; −1.5 to −1.99 reflect severe drought, and values below −2 reflect extreme drought (McKee et al., 1993).

3. Results

3.1. Trends in NDVI time series data in 1982–2013

Our results from GIMMS and MODIS data showed that the 'Three North' region experienced a positive NDVI trend during the growing season (May to September) for both 1982–2000 and 2000–2013. Both least square regression and Sen's slope method exhibited similar spatial patterns (Fig. 2). Area with a positive NDVI trend increased significantly after 2000, so did the magnitude of the greening trend. Only 14.88% of the total vegetated area showed a significant greening trend according to the Mann–Kendall test ($\alpha = 0.1$) in 1982–2000 compared with 37.80% in 2000–2013. The average increase of the NDVI for the entire vegetated area was 0.28%–0.38% yr^{-1} in 1982–2000 compared to 0.86%–1.12% yr^{-1} in 2000–2013. This continuous NDVI increase resulted in not only an increased vegetated area (growing season mean NDVI > 0.1) from 58.5% to 64.7% but also increased densely vegetated area (growing season mean NDVI > 0.5) from 9.68% to 16.59% during 1982–2000 to 2000–2013 (Fig. 3). We also analyzed the NDVI increase for different densities of vegetation. The results showed that all vegetation densities exhibited positive trends in both periods (Fig. 4). The fastest increase occurred in sparsely and moderately vegetated areas (growing season NDVI between 0.3 and 0.5) because afforestation was mainly implemented in these regions. These findings were confirmed with the GIMMS 3g dataset but the regression slope and significance were different (Figs. S1–3). The greening trend for all the vegetation densities increased significantly in the second period compared to the first. This can be attributed to the subsequent multiple afforestation programs and continued growth of previously planted trees.

The result from the BFAST analysis also showed an increase in greenness over time (Fig. 5). And this greening trend more than doubled after 2000. The causes of the two break points (circa 2000 and 2010) are difficult to determine because the expansive 'Three North' region has varying climatic conditions. The Asian monsoon has a large impact on the eastern part of the region, while it has limited effects in the west (Yu et al., 2014). We applied the BFAST analysis to the four subregions (Fig. S4). The break point in 2000 was caused by the abrupt decrease in the WNS, NNS and LPS possibly due to the continuous precipitation deficit in these region (Wang et al., 2003). The break point in 2010 was caused by the decrease in the WNS, NNS, and MXS. Almost all of these subregions showed an increase in greenness between the break points.

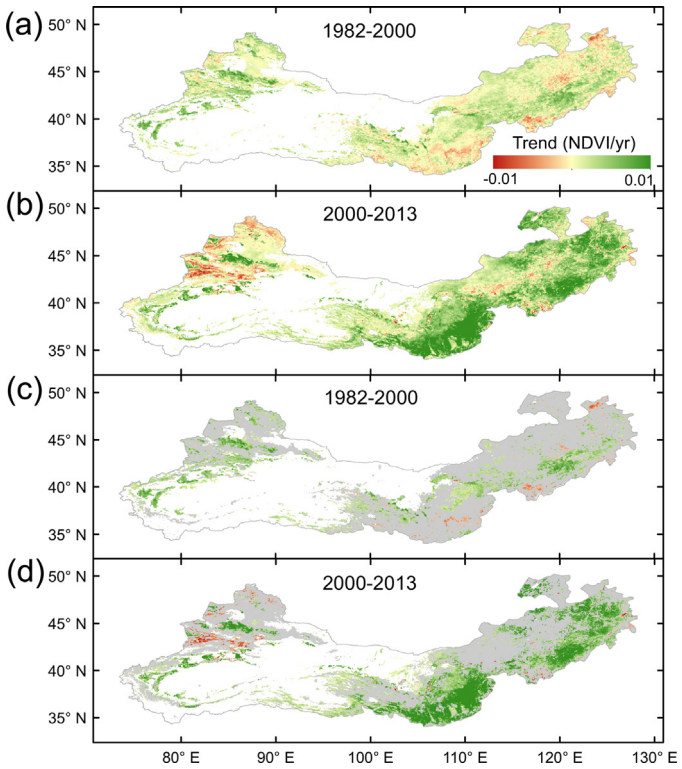

Fig. 2. NDVI trends during 1982–2000 and 2000–2013 as derived from linear models (a and b) and M–K models (c and d). The gray areas represent no significant trend using the M–K test, the white areas represent bare ground, with a mean NDVI less than 0.1 in the growing season (May to September).

3.2. Identifying key driving factors for increased NDVI greenness

During the past three decades, the average temperature of the growing season significantly increased (0.049 °C yr^{-1}, $P < 0.001$), while the precipitation slightly decreased (−0.025 mm yr^{-1}, $P > 0.965$) (Fig. S5). In fact, all four subregions experienced increasing temperatures ranging from 0.032 to 0.055 °C yr^{-1}. The precipitation in the LPS and MXS slightly increased (0.71 mm yr^{-1} and 0.32 mm yr^{-1}, respectively), while the two other eastern subregions' precipitation decreased (−1.93 mm yr^{-1} and −1.42 mm yr^{-1}). The increased temperature, along with the relatively low precipitation, made this region even drier and unsuitable for vegetation, especially trees to grow naturally (Dai, 2012; Gao et al., 2013; Peng et al., 2011).

To determine whether this greening trend was caused by phenological changes, we also calculated the changes in start of the season (SOS) and length of the growing season (LGS) for both periods. An advanced SOS and extended LGS were not prevalent in either period according to our analysis using GIMMS and MODIS data (Fig. 6), which is also confirmed by previous research (Cong et al., 2013; Wu and Liu, 2013). Some studies even showed a significant postpone of the SOS from 1998 to 2005 when the vegetation activity significantly increased (Wu and Liu, 2013; Yu et al., 2013). If we compare the trend of vegetation growth with phenological change spatially, the growth trend did not show close correlation

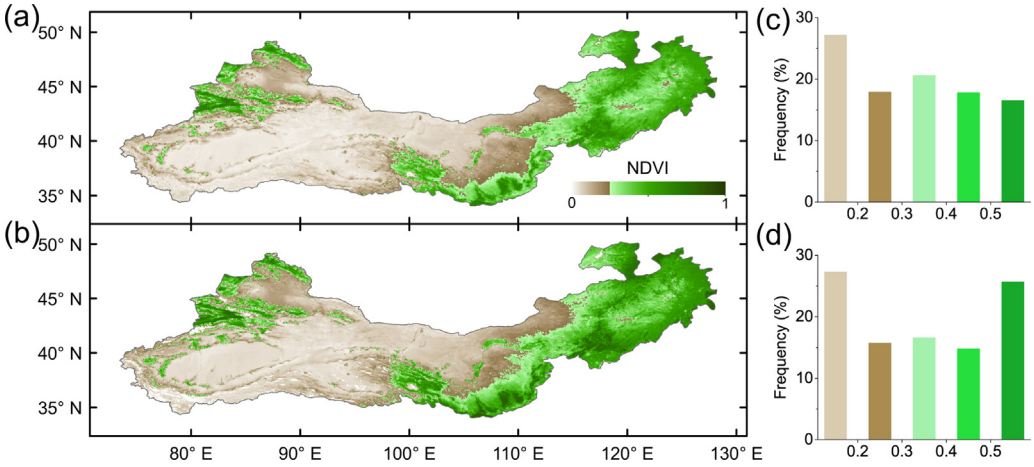

Fig. 3. Mean NDVI for the two periods during the growing season. (a) and (c) are the spatial distribution and frequency distribution, respectively, of the mean NDVI from 1982 to 1999. (b) and (d) are the spatial distribution and frequency distribution, respectively, of the mean NDVI from 2000 to 2013.

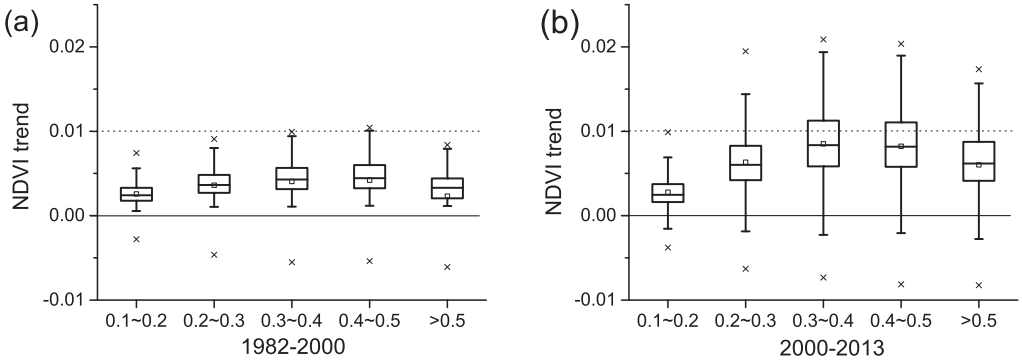

Fig. 4. Boxplot of Sen's slope for five NDVI categories for the 1982–2000 (a) and 2000–2013 (b) periods. The five NDVI categories represent the mean growing season NDVI for the corresponding period, which is shown in Fig. 3.

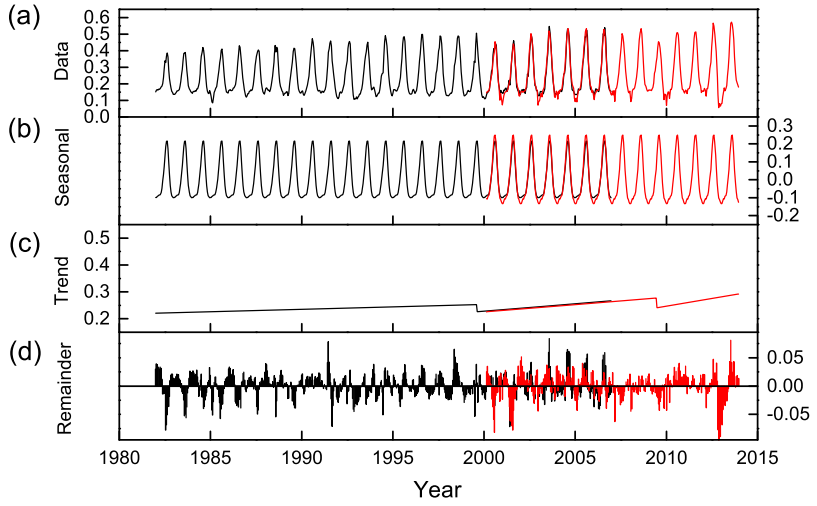

Fig. 5. The BFAST seasonal trend analysis of the NDVI in the Three North region in 1982–2006 from GIMMS (black) and in 2000–2013 from MODIS (red). (a) The NDVI time series of the two NDVI datasets. (b) The seasonal variability component derived from the BFAST model. (c) The trend component from the BFAST model; only the most significant abrupt change was detected for each dataset. (d) The remainder shows the variation of the NDVI after the removal of the seasonal and trend components in the time series. The bare ground was screened for analysis. (For interpretation of the references to color in this figure legend, the reader is referred to the web version of this article.)

with SOS ($R = 0.058$ and $n = 43\,277$ for 1982–2000; $R = -0.16$ and $n = 36\,308$ for 2000–2013) nor with the prolonged LGS trend ($R = -0.039$ and $n = 43\,277$ for 1982–2000; $R = 0.20$ and $n = 36\,308$ for 2000–2013). We also calculated the correlation between annual growing season mean NDVI and LGS for each pixel (Fig. 6(b, d)), most area showed a negative correlation for the first period, indicating that the shortened LGS did not necessarily lead to a decrease in growing season mean NDVI. Some of the area showed a positive correlation in the second period, however, only a small area in NNS and WNS also experienced an increase of vegetation activity. In

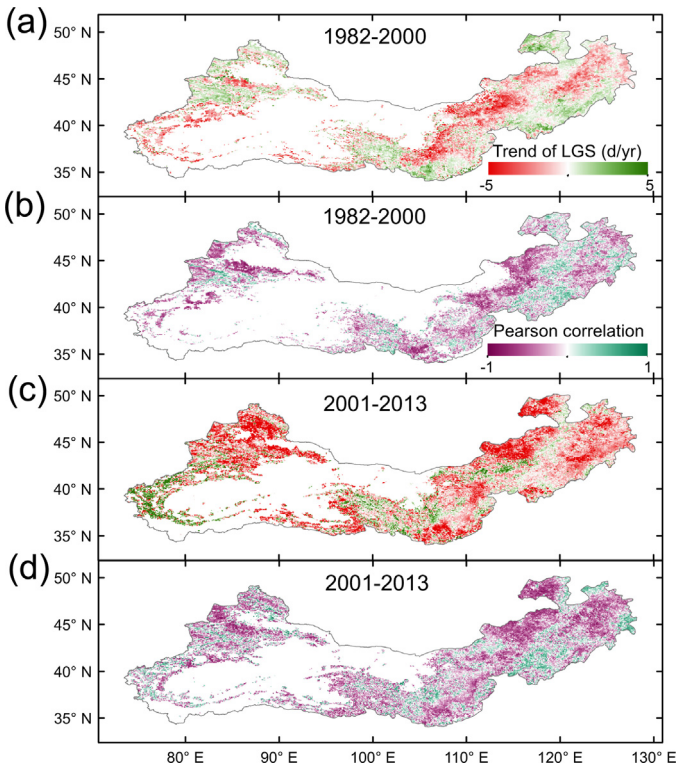

Fig. 6. (a) and (c) show the LGS trend for 1982–2000 and 2001–2013, respectively. Positive values indicate an extended LGS. (b) and (d) show the correlation between LGS and growing season mean NDVI for each year. Positive values indicate that the vegetation activity during the growing season positively respond to the LGS. Because the SOS shows a similar trend with LGS, the graph is not shown here.

addition, more that 95% of the correlation is not significant ($\alpha = 0.05$). The result from the GIMMS 3g dataset showed a similar trend for the phenological change, but the correlation is more prevailingly negative for both period (Fig. S6). For instance, the SOS and LGS were postponed and reduced in the LPS, where the most significant greenness increase occurred during 2000–2013. These findings indicated that phenological changes were not the major cause of the accelerated vegetation growth.

To understand this accelerating greening trend in the 'Three North' region, we also collected afforestation data from the China Forestry Yearbook (China Forestry Administration, 1985–2012). We found an acceleration in afforested areas during the past three decades (Fig. 1(c)). In addition to the TNSDP, three other afforestation programs were implemented between 1993 and 1999. The annual afforested area nearly doubled from 1.28 million ha before 2000 to 2.40 million ha after 2000. In addition, the GTGP also planted grass in areas that are not suitable for planting trees. These areas, which cover 1.78 million Ha, are not taken into account in Fig. 1(c).

4. Discussions

The greening trend during 1982–2000 is most significant ($12.66–17.54 \times 10^{-4}$ NDVI yr^{-1}) in the MXS because it has the largest farmland-protective forest network (Table 1). These trees, altogether covering 2.54 million ha, are usually planted in a line, which divides the farmland into blocks. However, they are difficult to map because so sparsely planted (Zheng et al., 2013). With milder living conditions and adequate water availability, these trees have a much higher survival rate. The 21.53 million ha of farmland under protection (65% of the total farmland in the 'Three North' region) and the sparse trees contribute to the NDVI increase of the entire

Table 1
Vegetation growth rate estimated by Sen's slope, linear regression and the BFAST model for the four subregions, the Three North region, southern China, and entire China. The trends are in 10^{-4} NDVI yr^{-1}.

	1982–2000			2000–2013		
	Sen's slope	Linear	BFAST	Sen's slope	Linear	BFAST
WNS	6.66	8.64	7.71	31.73	44.30	7.08*(47.8)
NNS	9.40	14.65	15.7*	39.72	52.20	27.3*(66.9)
LPS	3.84	3.88	10.4*	71.94	83.28	49.2*(26.7)
MXS	12.66	17.54	9.39**	17.12	24.16	11.7**(−2.03)
North	9.58	12.98	7.18	30.79	40.20	17.4*(23.8)
South	0.39	−0.09		5.62	8.85	
China	2.66	2.84		13.32	15.17	

For the first period, 1982–2000, only the GIMMS NDVI dataset was used. For 2000–2013, both MODIS and GIMMS datasets were used in the BFAST model, and only MODIS is used for Sen's slope and linear methods. The numbers in parentheses indicate the trends estimate by the GIMMS data for 2000–2006. Because the BFAST method contains abrupt changes between 1999 and 2000 in the trend analysis for the WNS, NNS, LPS and the entire Three North region; therefore, the BFAST trend before or after 2000 is actually the trend before or after the break point around 2000. For the Sen's slope method, the trend was averaged for the entire vegetated area for a comparison with the linear method (growing season average NDVI > 0.1).

* Indicates linear regression model was used with one break point.

** Indicates linear regression model was used with two break points.

'Three North' region. The water supply in the MXS mainly comes from rivers and melting snow on numerous mountains, not from precipitation (Deng et al., 2006). The increasing temperatures over the past three decades have increased the water supply and more water was utilized for irrigation (Chen et al., 2006). The benefits to the LPS were lowest during 1982–2000 because the least amount of forest was planted in this region, and a large area of natural forest north of the Ziwu Mountains and Huanglong Mountains was destroyed by farmland reclamation. During the second period, from 2000 to 2013, the greening trend increased nearly 40 folds in the LPS. In the other subregions, this increase also doubled or tripled. The GTGP was the major contributor to this increase because it was first implemented in the LPS and then extended across the country (Liu et al., 2013). In addition, the GTGP was most effective in the LPS because the largest area of sloping farmland was converted to forest. This is also expressed as the steep increase of the trend component in the BFAST analysis after 2000 (Fig. S4(c)). BSSCP received a large amount of investment to fight against the sandstorm and has the highest afforestation intensity. The significant increase of greening trend in NNS after 2000 confirmed the investment. However, due to the increased drought frequency and urbanization, the greening trend may have been partially offset, especially in the Beijing Tianjin urban area (Shan et al., 2015; Wu et al., 2014). The MXS benefited the least from the three programs and therefore maintained its original greening speed.

Although the GTGP and NFCP were implemented countrywide, 56.3% of the GTGP area and 42.0% of the NFCP area were included in our study region. If we do not take the large area of barren land into consideration, then the plant area ratio (afforested area/total vegetated area, an indicator of the afforest intensity) of the 'Three North' region was approximately 2.63-fold of the other regions in China where the GTGP was implemented, and this rate was 1.48 for NFCP. Additionally, planting trees in the 'Three North' region showed a higher increase in NDVI because of the relatively lower NDVI baseline. For these reasons, the greening trend was much higher in the 'Three North' region than in other regions of the country or even over the Asia-Pacific region (Chen et al., 2014).

Increasing investments and applicable policies also contributed to the effectiveness of these programs. The average subsidy for planting forests was 53.1 yuan/ha in 1978–1985 compared to 1875.8 yuan/ha in 2000–2007 for the TNSDP. However, the estimated cost may be approximately 6000 yuan/ha, which was still much higher than the investment (China Forestry Administration,

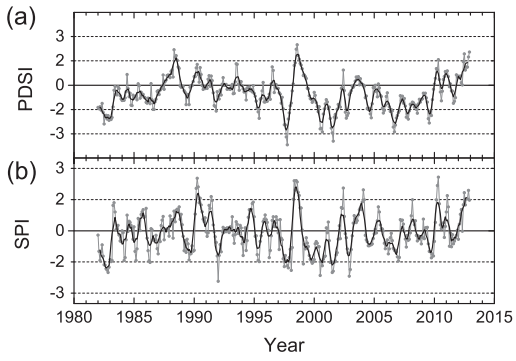

Fig. 7. The Palmer Drought Severity Index (PDSI) (a) and Standardized Precipitation Index (SPI) (b) for the Three North region. The solid line shows the mean value over 5 months.

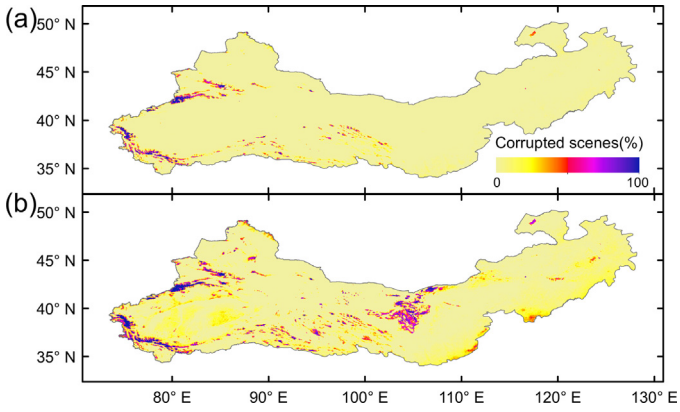

Fig. 8. The percentages of cloud-corrupted (a) and aerosol-corrupted (b) scenes for growing seasons from 2000 to 2013. All 98 16-day composites were used.

2008). The average investment for tree planting was 4500 yuan/ha in the Yellow River Basin for the GTGP, and higher investments resulted in better outcomes. Moreover, except for the Farmland Protective Forest Network, the TNSDP usually planted trees in dry regions to fight against desertification, which leaded to a much higher mortality rate. It was reported that only 15% of the planted trees survived (Cao, 2008). In contrast, the GTGP and NFCP planted trees in the southern part of the 'Three North' region, with higher water availability and a milder climate. The Chinese government also accumulated experience in implementing these programs and make proper adjustments: during the first few decades of the TNSDP, workers received little money and were not responsible for the survival rates; by contrast, the GTGP gave subsidies to workers only when the trees survived and began to grow. Therefore, workers are more careful with the planted trees and these new programs are more effective.

These ecological restoration programs have been in place for many years and have offered immense ecological, social and economic benefits (Deng et al., 2014; Feng et al., 2013; Liu et al., 2008; Wu et al., 2013). Afforestation in these regions accelerated the ecosystem succession from farmland or barren land to grassland and forest. It may have further changed the direction of this succession. For instance, in some semi-arid regions in the Loess Plateau, where there is no human intervention, the targeted ecosystem may be grassland or shrubland. However, the planted forests are growing well under human management and protection, and become dominant in this region. Challenges will also emerge if the regional climate becomes more complex under global warming. The two drought indices showed different trends after 2000. The PDSI continuously dropped below zero, while the SPI indicated that incoming precipitation did not significantly decrease (Fig. 7). This may be caused by the increasing transpiration from the planted trees and the consequent surface water imbalance (Jiang and Liang, 2013; Jiang et al., 2015). Semi-arid ecosystems are exhibiting a critical role in interannual variability of global carbon cycle (Poulter et al., 2014). However, increasing drought and flood frequencies, along with a high risk of pests and diseases due to monoculture (i.e., the presence of a single tree species), all contribute to the highly uncertain fate of these forests (Dale et al., 2001; Song et al., 2009). With increasing difficulty of afforestation in these areas due to less suitable land and water availability; how to maintain and promote the growth of these planted forests is an ongoing challenge.

Although the two NDVI datasets (GIMMS and MODIS) were acquired from different satellite series, they were recommended to be used in conjunction because of the good performance in both trends analysis and individual NDVI measurements (Guay et al., 2014). Another study also indicated these two datasets are highly comparable in north China (Fensholt and Proud, 2012). Using the BFAST analysis, the average NDVI from both GIMMS and MODIS maintained strong consistency during the growing season for the overlapping period (Fig. 5(a)). In addition, the trends were all calculated within each dataset to prove their reliability. In our study, the GIMMS 3g dataset showed a similar greening trend for both periods, but slightly different magnitude and the correlation between growing season mean NDVI and LGS. This could be due to the difference of temporal span for the second period and product algorithms. A previous study indicated that the land degradation at the beginning and the end of the time series will be hard to detect by trend analysis methods (Wessels et al., 2012). This also happened in our study. The positive reminder in Fig. 5(d) after 2012 indicated that the greening trend is slightly underestimated otherwise should be more evident. Data quality was checked using the MODIS QA layer (Fig. 8). The data quality for most area was very high in our study; only some mountainous regions were corrupted by cloud cover, and some desert areas were corrupted by aerosols. These corrupted areas mainly existed in the MXS. Admittedly, our study did not directly quantify the human effect on the vegetation growth trend, but a recent study which used remote sensed LAI and process-based model to separate the effect from natural environment change and human intervention also highlighted the importance of afforestation in northern China (Piao et al., 2015).

5. Conclusion

Our results presented in this study suggested that the greening trend continues to increase in the 'Three North' region of China during the past three decades. This increase in NDVI was much faster than any other regions in China and even in the Asia-Pacific region. Given the fact that this trend may not directly associated with phenological change and increase in water stress, the achievement of multiple ecological restoration programs may have greatly contribute to this vegetation activity increase in the 'Three North' regions.

Acknowledgements

This study was funded by the National Basic Research Program of China (2013CB956602) and the Natural Sciences and Engineering Research Council of Canada Discovery Grant. This work was conducted in China during the sabbatical leave of C. Peng.

Appendix.

Calculation of Mann–Kendall test and Sen's slope

The Mann–Kendall test is calculated as Eq. (2)

$$S = \sum_{i=1}^{n-1} \sum_{j=i+1}^{n} sgn(x_j - x_i) \quad (2)$$

where n is the number of the data, x_i and x_j are the data values in the time series i and j ($j > i$), respectively, and $sgn(x_i - x_j)$ is calculated as Eq. (3)

$$sgn(x_j - x_i) = \begin{cases} +1, & \text{if } x_j - x_i > 0 \\ 0 & \text{if } x_j - x_i = 0 \\ -1, & \text{if } x_j - x_i < 0 \end{cases} \quad (3)$$

The standardized normal test Z_s is calculated as Eq. (4)

$$Z_s = \begin{cases} \dfrac{S-1}{\sqrt{Var(S)}}, & \text{if } S > 0 \\ 0, & \text{if } S = 0 \\ \dfrac{S+1}{\sqrt{Var(S)}}, & \text{if } S < 0 \end{cases} \quad (4)$$

where the variance is computed when $n > 10$ as Eq. (5)

$$Var(S) = \frac{n(n-1)(2n+5)}{18} \quad (5)$$

where n is the number of the data; equal values are not considered in our study. A positive Z_s indicates an increasing trend, while a negative Z_s indicates a decreasing trend (Mann, 1945).

Sen's slope is calculated as Eq. (6)

$$\text{Sen's slope} = \text{Median}\left(\frac{x_j - x_i}{j - i}\right) \forall i < j \quad (6)$$

where x_i and x_j are the ith and ith values of the data, respectively (Sen, 1968).

Appendix B. Supplementary data

Supplementary data associated with this article can be found, in the online version, at http://dx.doi.org/10.1016/j.ecolind.2015.09.041.

References

Alcaraz-Segura, D., Chuvieco, E., Epstein, H.E., Kasischke, E.S., Trishchenko, A., 2010. Debating the greening vs. browning of the North American boreal forest: differences between satellite datasets. Glob. Change Biol. 16, 760–770.

Cao, S., 2008. Why large-scale afforestation efforts in China have failed to solve the desertification problem. Environ. Sci. Technol. 42, 1826–1831.

Cao, S., Wang, G., Chen, L., 2010. Questionable value of planting thirsty trees in dry regions. Nature 465, 31.

Chen, B., Xu, G., Coops, N.C., Ciais, P., Innes, J.L., Wang, G., Myneni, R.B., Wang, T., Krzyzanowski, J., Li, Q., Cao, L., Liu, Y., 2014. Changes in vegetation photosynthetic activity trends across the Asia–Pacific region over the last three decades. Remote Sens. Environ. 144, 28–41.

Chen, Y., Takeuchi, K., Xu, C., Chen, Y., Xu, Z., 2006. Regional climate change and its effects on river runoff in the Tarim Basin, China. Hydrol. Process. 20, 2207–2216.

China Forestry Administration, 1985–2012. China Forestry Yearbook. China Forestry Press, Beijing.

China Forestry Administration, Bureau of Three North Shelterbelt Development Program, 1987. Basic Manual of the Three North Shelterbelt Development Program. China Forestry Administration, Bureau of Three North Shelterbelt Development Program, Beijing.

China Forestry Administration, 2008. Development Report for the Three-North Shelterbelt System in the Past 30 Years: 1978–2008. China Forestry Press, Beijing.

Cong, N., Wang, T., Nan, H., Ma, Y., Wang, X., Myneni, R.B., Piao, S., 2013. Changes in satellite-derived spring vegetation green-up date and its linkage to climate in China from 1982 to 2010: a multimethod analysis. Glob. Change Biol. 19, 881–891.

Dai, A., 2012. Increasing drought under global warming in observations and models. Nat. Clim. Change 3, 52–58.

Dale, V.H., Joyce, L.A., McNulty, S., Neilson, R.P., Ayres, M.P., Flannigan, M.D., Hanson, P.J., Irland, L.C., Lugo, A.E., Peterson, C.J., 2001. Climate change and forest disturbances: climate change can affect forests by altering the frequency, intensity, duration, and timing of fire, drought, introduced species, insect and pathogen outbreaks, hurricanes, windstorms, ice storms, or landslides. BioScience 51, 723–734.

de Jong, R., de Bruin, S., de Wit, A., Schaepman, M.E., Dent, D.L., 2011. Analysis of monotonic greening and browning trends from global NDVI time-series. Remote Sens. Environ. 115, 692–702.

Deng, L., Liu, G.b., Shangguan, Z.p., 2014. Land-use conversion and changing soil carbon stocks in China's 'Grain-for-Green' Program: a synthesis. Glob. Change Biol. 20, 3544–3556.

Deng, X.-P., Shan, L., Zhang, H., Turner, N.C., 2006. Improving agricultural water use efficiency in arid and semiarid areas of China. Agric. Water Manag. 80, 23–40.

Falkowski, P., Scholes, R.J., Boyle, E., Canadell, J., Canfield, D., Elser, J., Gruber, N., Hibbard, K., Högberg, P., Linder, S., Mackenzie, F.T., Moore III, B., Pedersen, T., Rosenthal, Y., Seitzinger, S., Smetacek, V., Steffen, W., 2000. The global carbon cycle: a test of our knowledge of earth as a system. Science 290, 291–296.

Fan, B., Guo, L., Li, N., Chen, J., Lin, H., Zhang, X., Shen, M., Rao, Y., Wang, C., Ma, L., 2014. Earlier vegetation green-up has reduced spring dust storms. Sci. Rep. 4, 6749.

Feng, X., Fu, B., Lu, N., Zeng, Y., Wu, B., 2013. How ecological restoration alters ecosystem services: an analysis of carbon sequestration in China's Loess Plateau. Sci. Rep., 3.

Fensholt, R., Proud, S.R., 2012. Evaluation of earth observation based global long term vegetation trends—comparing GIMMS and MODIS global NDVI time series. Remote Sens. Environ. 119, 131–147.

Gao, T., Yang, X.C., Jin, Y.X., Ma, H.L., Li, J.Y., Yu, H.D., Yu, Q.Y., Zheng, X., Xu, B., 2013. Spatio-temporal variation in vegetation biomass and its relationships with climate factors in the Xilingol Grasslands, Northern China. PLOS ONE, 8.

Guay, K.C., Beck, P.S., Berner, L.T., Goetz, S.J., Baccini, A., Buermann, W., 2014. Vegetation productivity patterns at high northern latitudes: a multi-sensor satellite data assessment. Glob. Change Biol. 20, 3147–3158.

He, B., Chen, A., Wang, H., Wang, Q., 2015. Dynamic response of satellite-derived vegetation growth to climate change in the Three North shelter forest region in China. Remote Sens. 7, 9998–10016.

Huete, A., Didan, K., Miura, T., Rodriguez, E.P., Gao, X., Ferreira, L.G., 2002. Overview of the radiometric and biophysical performance of the MODIS vegetation indices. Remote Sens. Environ. 83, 195–213.

Jönsson, P., Eklundh, L., 2004. TIMESAT – a program for analyzing time-series of satellite sensor data. Comput. Geosci. 30, 833–845.

Jia, X., Fu, B., Feng, X., Hou, G., Liu, Y., Wang, X., 2014. The tradeoff and synergy between ecosystem services in the Grain-for-Green areas in Northern Shaanxi, China. Ecol. Indicators 43, 103–113.

Jiang, B., Liang, S., 2013. Improved vegetation greenness increases summer atmospheric water vapor over Northern China. J. Geophys. Res.: Atmos. 118, 8129–8139.

Jiang, B., Liang, S., Yuan, W., 2015. Observational evidence for impacts of vegetation change on local surface climate over northern China using the Granger causality test. J. Geophys. Res.: Biogeosci. 2014, JG002741.

Kendall, M.G., 1975. Rank Correlation Methods, 4th ed. Charles Griffin, London.

Kilpatrick, K., Podestá, G., Walsh, S., Williams, E., Halliwell, V., Szczodrak, M., Brown, O., Minnett, P., Evans, R., 2015. A decade of sea surface temperature from MODIS. Remote Sens. Environ. 165, 27–41.

Li, M.-m., Liu, A.-t., Zou, C.-j., Xu, W.-d., Shimizu, H., Wang, K.-y, 2012. An overview of the "Three-North" Shelterbelt project in China. For. Stud. China 14, 70–79.

Liu, D., Chen, Y., Cai, W., Dong, W., Xiao, J., Chen, J., Zhang, H., Xia, J., Yuan, W., 2014. The contribution of China's Grain to Green Program to carbon sequestration. Landsc. Ecol. 29, 1675–1688.

Liu, J., Diamond, J., 2005. China's environment in a globalizing world. Nature 435, 1179–1186.

Liu, J., Li, S., Ouyang, Z., Tam, C., Chen, X., 2008. Ecological and socioeconomic effects of China's policies for ecosystem services. Proc. Natl. Acad. Sci. 105, 9477–9482.

Liu, L., Tang, H., Caccetta, P., Lehmann, E.A., Hu, Y., Wu, X., 2013. Mapping afforestation and deforestation from 1974 to 2012 using Landsat time-series stacks in Yulin District, a key region of the Three-North Shelter region, China. Environ. Monit. Assess. 185, 9949–9965.

Ma, H., Lv, Y., Li, H., 2013. Complexity of ecological restoration in China. Ecol. Eng. 52, 75–78.

Mann, H.B., 1945. Nonparametric tests against trend. Econom.: J. Econom. Soc., 245–259.

McKee, T.B., Doesken, N.J., Kleist, J., 1993. The relationship of drought frequency and duration to time scales. In: Proceedings of the 8th Conference on Applied Climatology, American Meteorological Society Boston, MA, pp. 179–183.

Nemani, R.R., Keeling, C.D., Hashimoto, H., Jolly, W.M., Piper, S.C., Tucker, C.J., Myneni, R.B., Running, S.W., 2003. Climate-driven increases in global terrestrial net primary production from 1982 to 1999. Science 300, 1560–1563.

Palmer, W.C., 1965. Meteorological Drought. US Department of Commerce, Weather Bureau, Washington, DC, USA.

Peng, S., Chen, A., Xu, L., Cao, C., Fang, J., Myneni, R.B., Pinzon, J.E., Tucker, C.J., Piao, S., 2011. Recent change of vegetation growth trend in China. Environ. Res. Lett. 6, 044027.

Peng, S., Piao, S., Ciais, P., Fang, J., Wang, X., 2010. Change in winter snow depth and its impacts on vegetation in China. Glob. Change Biol. 16, 3004–3013.

Peng, S.S., Piao, S., Zeng, Z., Ciais, P., Zhou, L., Li, L.Z., Myneni, R.B., Yin, Y., Zeng, H., 2014. Afforestation in China cools local land surface temperature. Proc. Natl. Acad. Sci. U.S.A. 111, 2915–2919.

Piao, S., Fang, J., Ciais, P., Peylin, P., Huang, Y., Sitch, S., Wang, T., 2009. The carbon balance of terrestrial ecosystems in China. Nature 458, 1009–1013.
Piao, S., Fang, J., Liu, H., Zhu, B., 2005. NDVI-indicated decline in desertification in China in the past two decades. Geophys. Res. Lett., 32.
Piao, S., Friedlingstein, P., Ciais, P., Zhou, L., Chen, A., 2006a. Effect of climate and CO_2 changes on the greening of the Northern Hemisphere over the past two decades. Geophys. Res. Lett., 33.
Piao, S., Fang, J., Zhou, L., Ciais, P., Zhu, B., 2006b. Variations in satellite-derived phenology in China's temperate vegetation. Glob. Change Biol. 12, 672–685.
Piao, S., Yin, G., Tan, J., Cheng, L., Huang, M., Li, Y., Liu, R., Mao, J., Myneni, R.B., Peng, S., Poulter, B., Shi, X., Xiao, Z., Zeng, N., Zeng, Z., Wang, Y., 2015. Detection and attribution of vegetation greening trend in China over the last 30 years. Glob. Change Biol. 21, 1601–1609, http://dx.doi.org/10.1111/gcb.12795.
Pinzon, J., Tucker, C., 2014. A non-stationary 1981–2012 AVHRR NDVI3g time series. Remote Sens. 6, 6929–6960.
Poulter, B., Frank, D., Ciais, P., Myneni, R.B., Andela, N., Bi, J., Broquet, G., Canadell, J.G., Chevallier, F., Liu, Y.Y., Running, S.W., Sitch, S., van der Werf, G.R., 2014. Contribution of semi-arid ecosystems to interannual variability of the global carbon cycle. Nature 509, 600–603.
Rahimi, S., Gholami Sefidkouhi, M.A., Raeini-Sarjaz, M., Valipour, M., 2015. Estimation of actual evapotranspiration by using MODIS images (a case study: Tajan catchment). Arch. Agron. Soil Sci. 61, 695–709.
Sen, P.K., 1968. Estimates of the regression coefficient based on Kendall's tau. J. Am. Stat. Assoc. 63, 1379–1389.
Shan, N., Shi, Z., Yang, X., Gao, J., Cai, D., 2015. Spatiotemporal trends of reference evapotranspiration and its driving factors in the Beijing–Tianjin Sand Source Control Project Region, China. Agric. For. Meteorol. 200, 322–333.
Sobrino, J., Julien, Y., 2011. Global trends in NDVI-derived parameters obtained from GIMMS data. Int. J. Remote Sens. 32, 4267–4279.
Song, L., Zhu, J., Yan, Q., 2009. Review on the shelter forest decline. Chin. J. Ecol. 28, 1684–1690.
Song, X., Peng, C., Zhou, G., Jiang, H., Wang, W., 2014. Chinese Grain for Green Program led to highly increased soil organic carbon levels: a meta-analysis. Sci. Rep., 4.
Sun, G., Zhou, G., Zhang, Z., Wei, X., McNulty, S.G., Vose, J.M., 2006. Potential water yield reduction due to forestation across China. J. Hydrol. 328, 548–558.
Tan, M., Li, X., 2015. Does the Green Great Wall effectively decrease dust storm intensity in China? A study based on NOAA NDVI and weather station data. Land Use Policy 43, 42–47.
Tucker, C.J., Pinzon, J.E., Brown, M.E., Slayback, D.A., Pak, E.W., Mahoney, R., Vermote, E.F., El Saleous, N., 2005. An extended AVHRR 8-km NDVI dataset compatible with MODIS and SPOT vegetation NDVI data. Int. J. Remote Sens. 26, 4485–4498.
Verbesselt, J., Hyndman, R., Newnham, G., Culvenor, D., 2010a. Detecting trend and seasonal changes in satellite image time series. Remote Sens. Environ. 114, 106–115.
Verbesselt, J., Hyndman, R., Zeileis, A., Culvenor, D., 2010b. Phenological change detection while accounting for abrupt and gradual trends in satellite image time series. Remote Sens. Environ. 114, 2970–2980.
Vermote, E., Vermeulen, A., 1999. Atmospheric Correction Algorithm: Spectral Reflectances (MOD09), ATBD Version., pp. 4.
Vitousek, P.M., Mooney, H.A., Lubchenco, J., Melillo, J.M., 1997. Human domination of Earth's ecosystems. Science 277, 494–499.
Wang, X.M., Zhang, C.X., Hasi, E., Dong, Z.B., 2010. Has the Three Norths Forest Shelterbelt Program solved the desertification and dust storm problems in arid and semiarid China? J. Arid Environ. 74, 13–22.
Wang, Z., Zhai, P., Zhang, H., 2003. Variation of drought over northern China during 1950–2000. J. Geogr. Sci. 13, 480–487.
Wessels, K.J., van den Bergh, F., Scholes, R.J., 2012. Limits to detectability of land degradation by trend analysis of vegetation index data. Remote Sens. Environ. 125, 10–22.
Wu, X., Liu, H., 2013. Consistent shifts in spring vegetation green-up date across temperate biomes in China, 1982–2006. Glob. Change Biol. 19, 870–880.
Wu, Z., Wu, J., He, B., Liu, J., Wang, Q., Zhang, H., Liu, Y., 2014. Drought offset ecological restoration program-induced increase in vegetation activity in the Beijing–Tianjin sand source region, China. Environ. Sci. Technol. 48, 12108–12117.
Wu, Z., Wu, J., Liu, J., He, B., Lei, T., Wang, Q., 2013. Increasing terrestrial vegetation activity of ecological restoration program in the Beijing–Tianjin Sand Source Region of China. Ecol. Eng. 52, 37–50.
Xu, L., Myneni, R.B., Chapin Iii, F.S., Callaghan, T.V., Pinzon, J.E., Tucker, C.J., Zhu, Z., Bi, J., Ciais, P., Tømmervik, H., Euskirchen, E.S., Forbes, B.C., Piao, S.L., Anderson, B.T., Ganguly, S., Nemani, R.R., Goetz, S.J., Beck, P.S.A., Bunn, A.G., Cao, C., Stroeve, J.C., 2013. Temperature and vegetation seasonality diminishment over northern lands. Nat. Clim. Change 3, 581–586.
Yang, X., Ci, L., 2008. Comment on "Why large-scale afforestation efforts in China have failed to solve the desertification problem". Environ. Sci. Technol. 42, 7722–7723.
Yao, Z., Li, J., Zhao, Z., 2015. Synergistic use of AIRS and MODIS for dust top height retrieval over land. Adv. Atmos. Sci. 32, 470–476.
Yin, R., Yin, G., 2010. China's primary programs of terrestrial ecosystem restoration: initiation, implementation, and challenges. Environ. Manag. 45, 429–441.
Yu, G., Chen, Z., Piao, S., Peng, C., Ciais, P., Wang, Q., Li, X., Zhu, X., 2014. High carbon dioxide uptake by subtropical forest ecosystems in the East Asian monsoon region. Proc. Natl. Acad. Sci. 111, 4910–4915.
Yu, Z., Liu, S., Wang, J., Sun, P., Liu, W., Hartley, D.S., 2013. Effects of seasonal snow on the growing season of temperate vegetation in China. Glob. Change Biol. 19, 2182–2195.
Zhang, F., Xing, Z., Rees, H.W., Dong, Y., Li, S., Meng, F., 2014. Assessment of effects of two runoff control engineering practices on soil water and plant growth for afforestation in a semi-arid area after 10 years. Ecol. Eng. 64, 430–442.
Zhang, G., Dong, J., Xiao, X., Hu, Z., Sheldon, S., 2012. Effectiveness of ecological restoration projects in Horqin Sandy Land. China based on SPOT-VGT NDVI data. Ecol. Eng. 38, 20–29.
Zheng, X., Zhu, J., Yan, Y., 2013. Estimation of farmland shelterbelt area in the Three-North Shelter/Protective Forest Program regions of China based on mulit-scale remote sensing data. Chin. J. Ecol. 32, 1355–1363.
Zhou, W., Lewis, B.J., Wu, S., Yu, D., Zhou, L., Wei, Y., Dai, L., 2014. Biomass carbon storage and its sequestration potential of afforestation under Natural Forest Protection Program in China. Chin. Geogr. Sci. 24, 406–413.